Plasmonic Effects of Dual Metal Nanoparticle Layers for High-Performance Quantum Dot Solar Cells

John Hong[a,b †], *Byung-Sung Kim*[b†], *Bo Hou*[c], *Yuljae Cho*[c], *Sang Hyo Lee*[c], *Sangyeon Pak*[d], *Stephen M. Morris*[b], *Jung Inn Sohn*[e], *SeungNam Cha*[d]*

[a] School of Materials Science and Engineering, Kookmin University, Seoul, 02707, Republic of Korea

[b] Department of Engineering Science, University of Oxford, Parks Road, Oxford, OX1 3PJ, United Kingdom

[c] Department of Engineering, University of Cambridge, Cambridge, CB3 0FA, United Kingdom

[d] Department of Physics, Sungkyunkwan University, Suwon, Gyeonggi-do, 16419, Republic of Korea

[e] Division of Physics and Semiconductor Science, Dongguk University-Seoul, Seoul, 04620, Republic of Korea

*Corresponding Author (Prof. SeungNam Cha) Email: chasn@skku.edu

[†] Those authors contributed equally to this work.

ABSTRACT

To improve quantum dot solar cell performance, it is crucial to make efficient use of the available incident sunlight to ensure that the absorption is maximized. The ability of metal nanoparticles to concentrate incident sunlight via plasmon resonance can enhance the overall absorption of photovoltaic cells due to the strong confinement that results from near-field coupling or far-field scattering plasmonic effects. Therefore, to simultaneously and synergistically utilize both plasmonic effects, the placement of different plasmonic nanostructures at the appropriate locations in the device structure is also critical. Here we introduce two different plasmonic nanoparticles, Au and Ag, to a colloidal PbS quantum dot heterojunction at the top and bottom interface of the electrodes for further improvement of the absorption in the visible and near-infrared spectral regions. The Ag nanoparticles exhibit strong scattering whereas the Au nanoparticles exhibit an intense optical effect in the wavelength region where the absorption of light of the PbS quantum dot is strongest. It is found that these dual-plasmon layers provide significantly improved short-circuit current and power conversion efficiency without any form of trade-off in terms of the fill factor and open-circuit voltage, which may result from the indirect contact between the plasmonic nanoparticles and colloidal quantum dot films.

Colloidal quantum dot (CQD) solar cells, which are an evolving class of photovoltaic system, are expected to be promising candidates for inexpensive, mass producible, and highly efficient optoelectronic and photovoltaic applications.[1-6] The versatile bandgap tunability and solution processability of CQDs can allow for the controlled tailoring of the solar power conversion efficiency (PCEs) of quantum dot solar cells (QDSCs) through a simple heterojunction structure.[7,8] As a result, recent studies on lead sulfide (PbS) QDSC technology have progressed rapidly resulting in the highest certified PCE performance.[9-11] This notable advance in the PCE has been largely attributed to the improvement in the surface functionalization of CQD films using short surface ligand elements[12-15] (such as thiols and halides) and the design of new device architectures involving interfacial layers,[16-18] which gradually decrease surface charge trapping and increase exciton dissociation ratios, respectively. For a further enhancement in the PCE, however, it has also been considered that increasing the absolute number of exciton charge carriers can also contribute significantly to the overall performance of CQD photovoltaics.

In this regard, there have been many studies that have focused on controlling the number of charge carriers in CQD photovoltaics. Improving the light absorption efficiency can generate more charge carriers by additionally harvesting incident photons.[19] Therefore, to increase the absorption efficiency, the thickness of the CQD film (the photovoltaic active layers) may also be an important factor as one might expect a larger photon conversion is obtained with thicker CQD films. However, for the simple junction device structure, the thickness of the CQD films cannot be easily adjusted. This is because the thickness of the CQD film is limited to a certain value (usually 200-300 nm for the PbS QDSCs) that is defined by the fixed carrier diffusion length, which can be calculated from the minority carrier of the CQD films.[20,21] It is therefore important to find an

alternative approach for increasing the overall light absorption efficiency without changing the thickness of the CQD film.

Introducing plasmonic nanostructures (usually metallic nanoparticles (MNPs)) in photovoltaic solar cells (silicon and organic solar cells) is an alternative approach to improving the overall light absorption efficiency, leaving the thickness of photovoltaic active layers unaltered. Small Au and Ag nanoparticles are the best and conventional candidates for plasmonic resonance effects in solar cells.[22-25] Especially, those nanoparticles in solar cells are understood to be responsible for two different plasmonic effects, which are the localized surface plasmon resonance (LSPR) excitation at plasmon frequency and the light scattering phenomena of incident light.[26] Those two effects can promote optical absorption by concentrated near field intensity and increase light travel time by scattering. In principle, large-sized silver (Ag) nanoparticles (> 50 nm) can are more appropriate for scattering effects, whereas the small-sized gold (Au) nanostructures (< 20 nm) can induce strong near-field oscillation effects.[27] Combining those two plasmonic effects in solar cells with the different size and sort of nanoparticles can synergistically improve the light absorption efficiency. Furthermore, to maximize the plasmonic effects, the placement of MNPs at the correct locations is also of critical importance for the enhancement of the overall device performance.[28-31] For example, a number of research groups have placed the plasmonic nanostructures within the photovoltaic active layers. However, it has been noted that, in some cases, the direct combination between the plasmonic nanostructures and the photovoltaic active films can, unintentionally, induce undesirable quenching of excitons along with fast carrier recombination: it is understood that in this case they act as charge carrier trap sites, resulting in a

low fill factor (*FF*) and PCE performance. Therefore, efficiently utilizing both plasmonic effects in proper locations is strongly required to improve the QDSC performance.

In this work, we aim to not only incorporate two different plasmonic nanostructures (Au and Ag nanoparticles) within a QDSC, but also to position these at the appropriate locations within the device so that both plasmonic effects can be exploited leading to enhanced energy conversion in the QDSCs. We readily apply two different nanoparticles (i.e. dual-plasmon layers) via a simple nanoparticle solution deposition process. By combining two different plasmon nanoparticles only at the interface of the CQD films, we can synergistically utilize both the near-field intensity coupling and the light scattering resonance effects. The large Ag nanoparticles (~ 50 nm) are placed on the hole transfer layers (the back position of light path in the devices) to maximize the large scattering effect whereas the small Au nanoparticles (~ 10 nm) are placed on the electron transfer layers (the front position of light path in the devices) to amplify the intensity of incident photons. Those NP positions were selectively decided due to their plasmonic effects. These dual-plasmon layers give rise to a significantly improved J_{sc} and PCE performance without any tradeoff in the *FF* and V_{oc}, which may result from the indirect contact between the plasmonic nanoparticles and the CQDs. Therefore, these dual-plasmonic layers are firstly applied to the QD photovoltaic application. Moreover, the employment of dual-metal nanoparticle layers will provide further insight into the development of ideal plasmonic quantum dot devices for future photovoltaic systems.

To verify the plasmonic effects on the QDSC, we insert the Au and Ag nanoparticles at the top and bottom of the interface layers in the QDSC junction structure, respectively. For the

fabrication of the PbS QDSCs, first, PbS QDs were synthesized and collected according to the processes described in our previous work.[32] Moreover, the bandgap of the PbS QDs was found to be 1.29 eV from the absorption spectrum of the PbS QD solution using an ultraviolet−visible spectrometer (UV−Vis), as shown in Figure S1a. The detailed fabrication and structure of the CQD solar cell devices with the two different plasmonic nanostructures are illustrated in Figure 1a. For the fabrication process, ZnO nanoparticles (which act as the electron transfer layers) were deposited on indium tin oxide (ITO)/glass substrates using a spin-coating method. On the as-prepared ZnO/ITO substrates, the Au nanoparticle (~ 10 nm) solution was spin-coated as the first plasmonic layer (Figure 1b). Subsequently, the PbS CQD films were spin-coated onto the Au layers and serve as the photovoltaic active layers. In the PbS active layers, tetrabutylammonium iodide (TBAI) and 1,2-ethanedithiol (EDT) ligand-treated PbS QD films were used, which are the most frequently employed surface ligands for PbS CQDs as they show high PCE and good stability amongst the different types of QD ligands that have been studied to date. A solid-state ligand exchange process was applied in order to substitute the initial long-chain oleic acid (OA) ligands for the short-chain TBAI and EDT ligands. After the 12 layers of the PbS CQD films (10 TBAI-treated layers and 2 EDT-treated layers, which is the best combination of QD p-n junction ratio in PbS QDSCs), the Ag nanoparticle solution was then spin-coated onto the device and served the purpose of being the second plasmonic layer to maximize the light absorption efficiency. The QDSCs were systematically fabricated such that excitons can dissociate into free carriers, and the electrons and holes can then be collected at each electrode.

The small size (~ 10 nm) of the Au nanoparticles at the front layer can be used as subwavelength antennas, in which the plasmonic near-field coupling of Au is strongly coupled

with phonons at ~ 500 nm wavelength. The large size (~ 50 nm) of the Ag nanoparticles at the back layer can be also used as far-field scattering source to trap the propagating light from the Sun into the CQD films, by folding effects. Therefore, the scattering effect that results from the Ag nanoparticles mainly serves to enhance the absorption of the CQD films over the range of light intensities (Figure 2a). The dual LSPR antenna and scattering effects will significantly increase the light absorption efficiency of the CQD films, subsequently boosting the overall performance of the CQD solar cells. Moreover, Figure S2 shows transmission electron microscopy images of the Au and Ag nanoparticles: Figure S2a and b show the silica-coated Au nanoparticles, which have a diameter of ~ 10 nm whereas Figure S2c and d confirm that the Ag nanoparticles have a diameter of ~ 50 nm.

In order to investigate the influence of the Au and Ag nanoparticles, atomic force microscopy (AFM) and ultraviolet-visible (UV-Vis) spectroscopy were carried out. Figure S3 shows AFM topography images of the Au and Ag nanoparticles for different concentrations, respectively. Most nanoparticles maintained a spherical and well-defined shape. The different concentration of the nanoparticles led to a change in the aerial deposition density. For an optimized performance, the small density of nanoparticles on the films might induce low plasmonic effects, and also the large density of nanoparticles can interfere with the carrier transport paths. The optical absorption enhancement by the nanoparticles has been investigated (Figure 2b and 2c). The redshift of absorption peak compared to Figure S1a-b is due to the ligand exchange method, which overlap and decrease the inter-particle distance of QDs. The CQD films prepared for the UV-Vis absorption analysis have the same thickness (5 layers of CQD films). There is no observable shift in the absorption peak after the deposition of the Au and Ag nanoparticles on the CQD films,

indicating that the applied nanoparticles do not change the optical properties of the CQD films. After the 2% Ag layers, the thick Ag layers might as the blocking layer. Interestingly, the Au nanoparticles applied onto the CQD films is found to selectively increase the absorption spectra over the wavelength range from ~ 450 – ~ 700 nm, but near the absorption edge region (900 – 1200 nm), the absorption spectra of the CQD film exhibits no significant change across the different concentrations of the applied Au nanoparticles, indicating that there is no spectral response of the Au nanoparticles. In contrast, the applied Ag nanoparticles are found to increase the absorption spectra of the CQD films over the full spectral range (450 – 1200 nm), which is in accordance with the scattering effect that is observed for the Ag nanoparticles.

To investigate the absorption enhancement of the CQD films with the application of the Au and Ag nanoparticles, we recorded the photocurrent density and voltage (*J-V*) curves when subjected to the standard AM 1.5G solar illumination (100 mW cm^{-2}). Figure 3a shows representative *J-V* curves of the reference (without Au and Ag nanoparticles) and Au plasmonic QDSCs (Au-QDSCs). The Au plasmonic nanoparticles applied to the QDSCs was found to lead to substantial improvement in the PCE from 7.22% to 8.32% at the optimized concentration. This significant enhancement in the PCE of the QDSC largely results from improvements in the short-circuit current (J_{sc}), fill factor (*FF)* and open-circuit voltage (V_{oc}). The Au nanoparticles trigger the near-field coupling plasmonic effect, and subsequently facilitate both light absorption as well as charge separation. Similarly, as shown in Figure 3b, the applied Ag nanoparticles also show a substantial improvement in the PCE reaching 8.12% for champion cells at the optimized concentration. In this case, the major PCE enhancement with the addition of the Ag nanoparticles results mainly from the improvement in the J_{sc} . The slight V_{oc} increase could be also associated

with the Au NP plasmonic couplings, promoting the electron transfer to the ZnO films and increasing the built-in potential of the QDSCs.[33-34] Figure S4 shows that the power conversion efficiency is decreased or not changed when the location of the Ag and Au particles are interchanged. This is because the reflection effects and large size of Ag nanoparticles, which are relocated at the front ZnO ETL, may block and reflect in-coming light to the cells, and also, the small Au particles, which are relocated at the back HTL, are not enough to induce the expected reflection effects on transferring out-going light in the cells. As shown in Figure S5, the lower J_0 (saturation current) value and steeper curve of the recombination regions indicate that the QDSCs with the Au NPs can show the higher V_{oc} than the bare QDSCs. Moreover, light trapping due to the presence of the plasmonic scattering effect over the entire wavelength range is found to increase the effective photon path length in the QDSCs.

We have measured the external quantum efficiency (EQE) of the QDSCs to determine the origin of the performance enhancement (Figure 3c and 3d). After applying the Au nanoparticles, the regions of the EQE spectra are selectively increased. The major increase in the EQE spectra with the wavelength region of ~ 400 nm – ~ 700 nm. However, for the region near 900 – 1200 nm, there are no significant spectral difference between the reference cell and the Au-QDSCs, which are in good agreement with the results obtained from UV-Vis. As shown in Figure 3d, the EQE spectra for the Ag-based plasmonic QDSCs (Ag-QDSCs) exhibits an increase in the area compared with that of the reference QDSCs, indicating a larger J_{sc} value for the Ag-QDSCs. The enhancement in the EQE have been made over the full wavelength range of incident photons on the CQD films by the scattering effect. The photovoltaic performance of the Au- and Ag-QDSCs are summarized in Figure 3e and 3f, respectively. The values of the PCE are increased depending

on the concentration of the applied Au and Ag nanoparticles, but a further increase in concentration beyond the optimized concentration results in a decrease in the PCE. This is because the greater concentration of Au and Ag nanoparticles can act as the blocking sites in the QDSCs. Figure S6 shows the dark *J-V* curves of QDSCs with the Au or Ag layers at the interfacial layers or middle layers, where the NPs are embedded in the PbS active layers. The inserted NPs in the PbS active layers result in the lower slope at injection region, which might be react as the trap sites in the active layers. The dark *J-V* results are well-matched with our initial assumption that the embedded NPs can react as the recombination sites which decrease the overall performance of QDSCs.

In the final experiment in this study, we applied both the Au and Ag nanoparticles to our solar cell to form dual-plasmonic layers so as to maximize both the antenna and scattering effects (Figure 4). From these results, it is found that the champion QDSCs with dual Au and Ag nanoparticle layers exhibits a V_{oc} = 0.54 V, J_{sc} = 26.16 mA cm^{-2}, *FF* = 0.65 and PCE = 9.18 % (Figure 4a). The increase in the V_{oc} and *FF* are strongly related to the antenna effects of the Au nanoparticles. Instead, the relatively large increase in the J_{sc} should be strongly correlated to the dual plasmonic effects by the enlarged number of charge carriers from the high photon absorption efficiency. Figure 4b and 4c also show statistical and detailed solar cell results for both the dual-plasmonic and reference cells (averaged over 15 devices). The QDSCs with dual-plasmonic layers show a 13% increase in the J_{sc}, a 4% increase in V_{oc}, and a 7% increase in *FF*, and finally a 25% enhancement in the PCE compared to the reference cell. Figure 4d shows the table with the average values of QDSCs. According to our experimental findings, the existence of the dual-plasmonic layers in the CQD photovoltaic system can effectively improve the PCE performance through an increase in the charge collection at short-wavelengths by the antenna effect of the Au nanoparticles

and across the full wavelength region by the Ag nanoparticles, as validated by the photovoltaic measurements.

In conclusion, we have demonstrated that the performance of QDSCs can be effectively manipulated by the plasmonic Au and Ag nanoparticles at proper locations on the CQD films. The Au and Ag nanoparticles can induce a near-field coupling resonance and light scattering resonance effects, respectively. These effects significantly enhance the overall photon absorption efficiency of the CQD films, leading to an improvement in the device performance. The optical absorption results also indicate that the applied Au and Ag nanoparticle layers can enhance the overall absorption efficiency. In doing so, the simultaneous utilization of both plasmonic effects in the QDSCs result in improved V_{oc} and J_{sc} at the expense of PCE values. An optimized solar cell can reach a PCE as high as 9.16%. The synergistically applied plasmonic effects in the CQD films is a promising technique for producing highly efficient CQD photovoltaics for a range of optoelectronic applications such as solar cells. Moreover, this approach can be used to help better understand energy harvesting dynamics when plasmonic effects are of importance in CQD films.

ACKNOWLEDGMENT

This work was supported by the National Research Foundation of Korea (NRF) (2019R1A2C1005930) and the European Commission Horizon 2020 under Grant Agreement Number 685758.

REFERENCES

[1] Bera D, Qian L, Tseng T-K, Holloway P (2010) Quantum dots and their multimodal applications: a review. Mater 3:2260–2345.

[2] Carey G, Abdelhady A, Ning Z, Thon S, Bakr O, Sargent E (2015) Colloidal quantum dot solar cells. Chem Rev 115:12732–12763.

[3] Kim J, Voznyy O, Zhitomirsky D, Sargent E (2013) 25th Anniversary article: colloidal quantum dot materials and devices: a quarter-century of advances. Adv Mater 25:4986–5010.

[4] Supran G, Song K, Hwang G, Correa R, Scherer J, Dauler E, Shirasaki Y, Bawendi M, Bulović V (2015) High-performance shortwave-infrared light-emitting devices using core–shell (PbS–CdS) colloidal quantum dots. Adv Mater 27:1437–1442.

[5] Semonin O, Luther J, Beard M (2012) Quantum dots for next-generation photovoltaics. Mater Today 15:508–515.

[6] Sargent E (2012) Colloidal quantum dot solar cells. Nat Photonics 6:133–135.

[7] Chuang C-H, Brown P, Bulović V, Bawendi M (2014) Improved performance and stability in quantum dot solar cells through band alignment engineering. Nat Mater 13:796–801.

[8] McDonald S, Konstantatos G, Zhang S, Cyr P, Klem E, Levina L, Sargent E (2005) Solution-processed PbS quantum dot infrared photodetectors and photovoltaics. Nat Mater 4:138–142.

[9] Liu M, Voznyy O, Sabatini R, Arquer P. de, Munir R, Balawi A, Lan X, Fan F, Walters G, Kirmani A, Hoogland S, Laquai F, Amassian A, Sargent E (2015) Hybrid organic–inorganic inks flatten the energy landscape in colloidal quantum dot solids. Nat Mater 16:258-263.

[10] Yang Z, Fan J, Proppe A, Arquer P de, Rossouw D, Voznyy O, Lan X, Liu M, Walters G, Quintero-Bermudez R, Sun B, Hoogland S, Botton G, Kelly S, Sargent E (2017) Mixed-quantum-dot solar cells. Nat Commun 8:1325.

[11] Lan X, Voznyy O, Arquer P de, Liu M, Xu J, Proppe A, Walters G, Fan F, Tan H, Liu M, Yang Z, Hoogland S, Sargent E (2016) 10.6% Certified colloidal quantum dot solar cells via solvent-polarity-engineered halide passivation. Nano Lett 16:4630–4634.

[12] Cao Y, Stavrinadis A, Lasanta T, So D, Konstantatos G (2016) The role of surface passivation for efficient and photostable PbS quantum dot solar cells. Nat Energy 1:16035.

[13] Azmi R, Oh S-H, Jang S-Y (2016) High-efficiency colloidal quantum dot photovoltaic devices using chemically modified heterojunctions. ACS Energy Lett 1:100–106.

[14] Kim B-S, Hong J, Hou B, Cho Y, Sohn J, Cha S, Kim J (2016) Inorganic-ligand exchanging time effect in PbS quantum dot solar cell. Appl Phys Lett 109:063901.

[15] Hong J, Hou B, Lim J, Pak S, Kim B-S, Cho Y, Lee J, Lee Y-W, Giraud P, Lee S, Park J, Morris S, Snaith H, Sohn J, Cha S, Kim J (2016) Enhanced charge carrier transport properties in colloidal quantum dot solar cells via organic and inorganic hybrid surface passivation. J Mater Chem A 4:18769–18775.

[16] Ren Z, Kuang Z, Zhang L, Sun J, Yi X, Pan Z, Zhong X, Hu J, Xia A, Wang J (2017) Enhancing electron and hole extractions for efficient PbS quantum dot solar cells. Solar RRL 1:1700176.

[17] Wang H, Kubo T, Nakazaki J, Segawa H (2017) Solution-processed short-wave infrared PbS colloidal quantum dot/ZnO nanowire solar cells giving high open circuit voltage. ACS Energy Lett 2:2110-2117.

[18] Cho Y, Giraud P, Hou B, Lee Y, Hong J, Lee S, Pak S, Lee J, Jang J, Morris S, Sohn J, Cha S, Kim J (2018) Charge transport modulation of a flexible quantum dot solar cell using a piezoelectric effect. Adv Energy Mater 8:1700809.

[19] Kim Y, Bicanic K, Tan H, Ouellette O, Sutherland B, Arquer P de, Jo J, Liu M, Sun B, Liu M, Hoogland S, Sargent E (2017) Nanoimprint-transfer-patterned solids enhance light absorption in colloidal quantum dot solar cells. Nano Lett 17:2349–2353.

[20] Rekemeyer P, Chuang C-H, Bawendi M, Gradecak S (2017) Minority carrier transport in lead sulfide quantum dot photovoltaics. Nano Lett 17:6221–6227.

[21] Cho Y, Hou B, Lim J, Lee S, Pak S, Hong J, Giraud P, Jang A-R, Lee Y-W, Lee J, Jang J, Snaith H, Morris S, Sohn J, Cha S, Kim J (2018) Balancing charge carrier transport in a quantum dot P-N junction toward hysteresis-free high-performance solar cells. ACS Energy Lett 3:1036–1043.

[22] Lu L, Luo Z, Xu T, Yu L (2013) Cooperative plasmonic effect of Ag and Au nanoparticles on enhancing performance of polymer solar cells. Nano Lett 13:59–64.

[23] Peng S, McMahon J, Schatz G, Gray S, Sun Y (2010) Reversing the size-dependence of surface plasmon resonances. Proc Natl Acad Sci 107:14530-14534.

[24] Guo Q, Zhang C, Hu X (2016) A spiral plasmonic lens with directional excitation of surface plasmons. Sci Rep 6:32345.

[25] Zhao F, Zhang C, Chang H, Hu X (2014) Design of plasmonic perfect absorbers for quantum-well infrared photodetection. Plasmonics 9:1397.

[26] Sharma M, Pudasaini P, Ruiz-Zepeda F, Vinogradova E, Ayon A (2014) Plasmonic effects of Au/Ag bimetallic multispiked nanoparticles for photovoltaic applications. ACS Appl Mater Interfaces 6:15472–15479.

[27] Stratakis E, Kymakis E (2013) Nanoparticle-based plasmonic organic photovoltaic devices. Mater Today 16:133-146.

[28] Kawawaki T, Wang H, Kubo T, Saito K, Nakazaki J, Segawa H, Tatsuma T (2015) Efficiency enhancement of PbS quantum Dot/ZnO nanowire bulk-heterojunction solar cells by plasmonic silver nanocubes. ACS Nano 9:4165–4172.

[29] Baek S, Song J, Choi W, Song H, Jeong S, Lee J (2015) A resonance-shifting hybrid n-type layer for boosting near-infrared response in highly efficient colloidal quantum dots solar cells. Adv Mater 27:8102–8108.

[30] Beck F, Stavrinadis A, Diedenhofen S, Lasanta T, Konstantatos G (2014) Surface plasmon polariton couplers for light trapping in thin-film absorbers and their application to colloidal quantum dot optoelectronics. ACS Photonics 1:1197–1205.

[31] Gonfa B, Kim M, Zheng P, Cushing S, Qiao Q, Wu N, Khakani M, Ma D (2016) Investigation of the plasmonic effect in air-processed PbS/CdS core–shell quantum dot based solar cells. J Mater Chem A 4:13071–13080.

[32] Hou B, Cho Y, Kim B, Hong J, Park J, Ahn S, Sohn J, Cha S, Kim J (2016) Highly monodispersed PbS quantum dots for outstanding cascaded-junction solar cells. ACS Energy Lett 1:834–839.

[33] Luo Q, Zhang C, Deng X, Zhu H, Li Z, Wang Z, Chen X, Huang S (2017) Plasmonic effects of metallic nanoparticles on enhancing performance of perovskite solar cells. ACS Appl Mater Interfaces 9:34821–34832.

[34] Hou B, Cho Y, Kim B-S, Ahn D, Lee S, Park J, Lee Y-W, Hong J, Im H, Morris S, Sohn J, Cha S, Kim J (2017) Red green blue emissive lead sulfide quantum dots: heterogeneous synthesis and applications. J Mater Chem C 5:3692–3698.

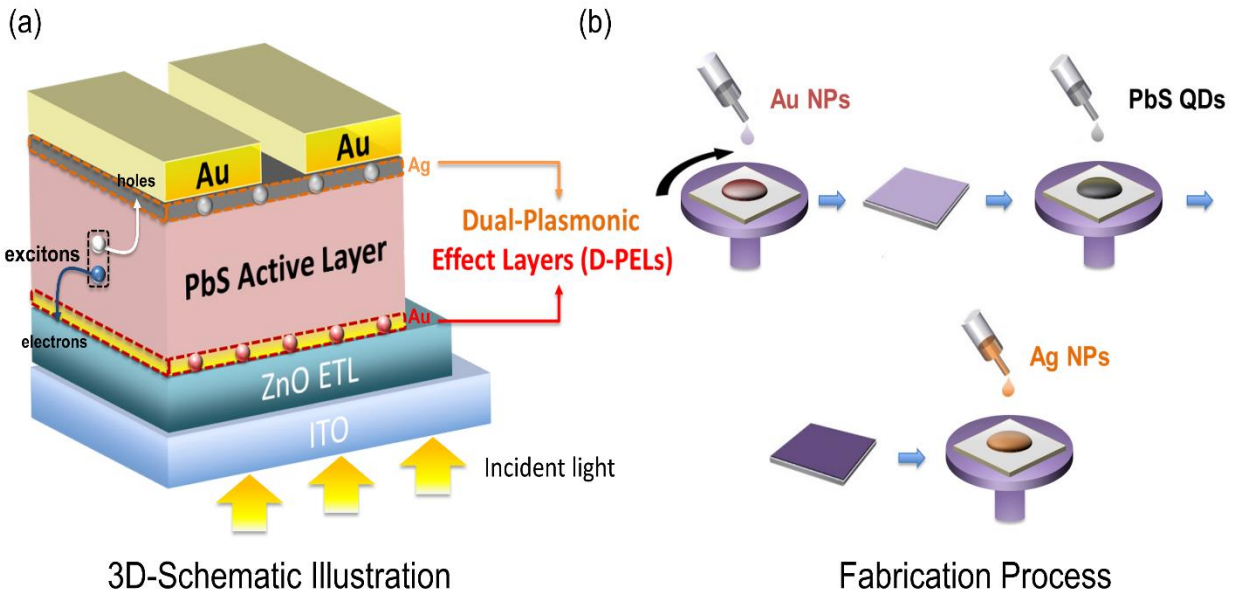

Figure 1. (a) Schematic illustration of the quantum dot solar cells with the dual-plasmonic effect layers. (b) Fabrication process of the quantum dot solar cells with the dual-plasmonic effect layers.

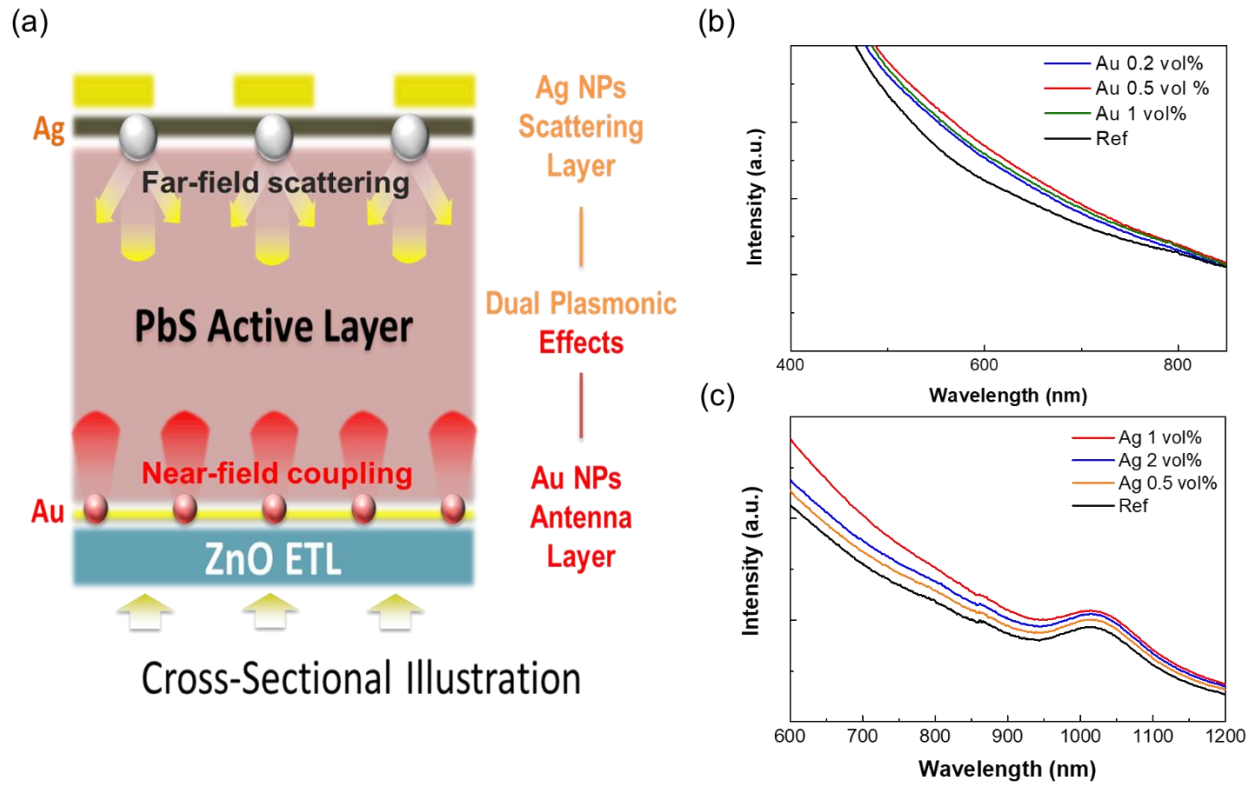

1

2 **Figure 2.** (a) Cross-sectional illustration of the quantum dot solar cells with the dual-plasmonic

3 effects. Ultraviolet–visible images of the PbS QD films with the (b) Au NPs and (c) Ag NPs.

4

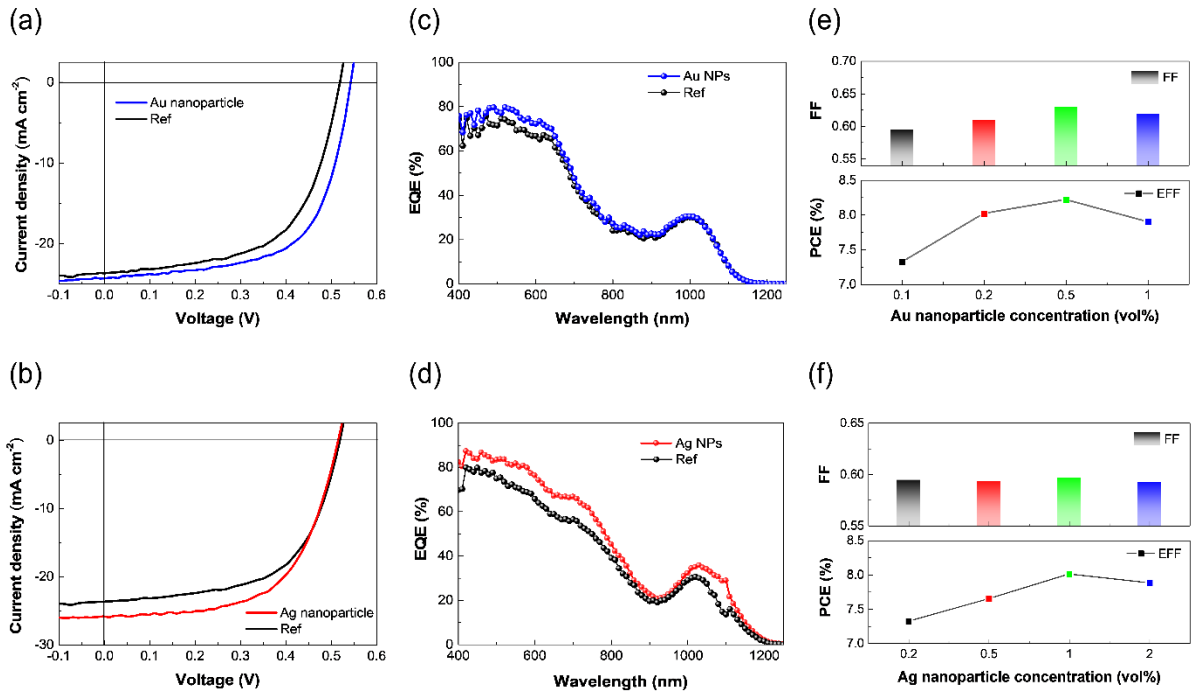

Figure 3. *J-V* curves of the QDSCs with the (a) Au NP layers and (b) Ag NP layers. External quantum efficiency images of the QDSCs with the (c) Au NP layers and (d) Ag NP layers. Overall *FF* and PCE performance of the QDSCs with the (e) Au NP layers and (f) Ag NP layers in the QDSCs.

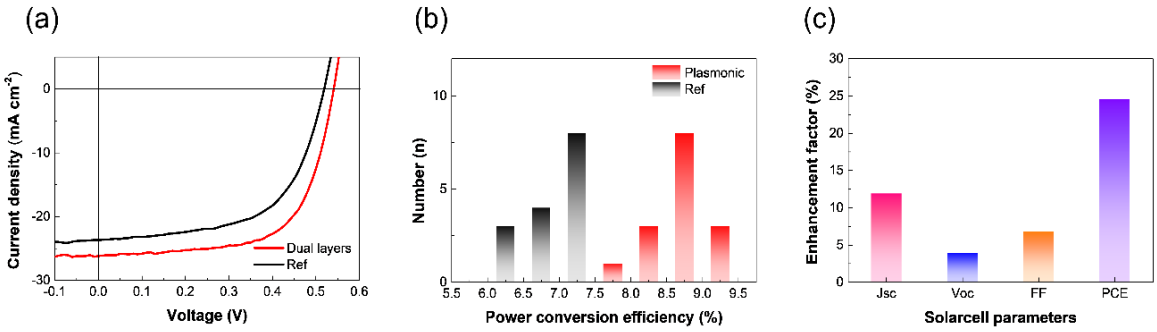

(d)

Parameters	Dual plasmonic cell	Reference cell
Jsc (mA cm^{-2})	26.05 ± 0.22 (26.16)	23.26 ± 0.39 (23.67)
Voc (V)	0.53 ± 0.01 (0.54)	0.51 ± 0.01 (0.52)
FF	0.62 ± 0.02 (0.65)	0.58 ± 0.02 (0.60)
PCE (%)	8.64 ± 0.35 (9.18)	6.93 ± 0.32 (7.38)

Figure 4. (a) *J-V* curves of the QDSCs with the dual-plasmonic effect layers (b) Overall PCE statistics of the QDSCs with and without the dual-plasmonic effect layers. (c) Enhancement factor of the QDSCs with the dual-plasmonic effect layers. (d) Performance table of the QDSCs.